

## RESEARCH ARTICLE

# A TENS Based System for 2-Dimensional Balance Biofeedback Under Muscle Fatigue Condition

JUNYEONG LEE<sup>1</sup>, HOSU LEE<sup>1</sup>, AMRE EIZAD<sup>2</sup>, AND JUNGWON YOON<sup>1</sup>, (Member, IEEE)

<sup>1</sup>School of Integrated Technology, Gwangju Institute of Science and Technology, Gwangju 61005, South Korea

<sup>2</sup>Center for Intelligent and Interactive Robotics, Korea Institute of Science and Technology, Seoul 02792, South Korea

Corresponding author: Jungwon Yoon (jyoon@gist.ac.kr)

This work was supported in part by the Gwangju Institute of Science and Technology (GIST) Research Institute GIST-Chonnam National University Hospital (CNUH) research collaboration and the “AI-based GIST Research Scientist Project” grants funded by GIST in 2022; in part by the National Research Foundation of Korea (NRF) under Grant 2019M3C1B8090798; and in part by the “Basic Science Research Program” of the NRF funded by the Ministry of Education, Republic of Korea under Grant 2022R1A6A3A01087395.

This work involved human subjects or animals in its research. Approval of all ethical and experimental procedures and protocols was granted by the Institutional Review Board of Gwangju Institute of Science and Technology, Gwangju, South Korea under Application No. 20210609-HR-61-07-04, and performed in line with the Declaration of Helsinki.

**ABSTRACT** Many balance assist or training systems have been developed to improve postural control, however these have limitations such as being bulky or unable to provide 2-dimensional feedback. Furthermore, efficiency of the commonly used vibro-tactile feedback modality can be reduced due to muscle fatigue. Therefore, we suggest a transcutaneous electrical nerve stimulation (TENS) based electro-tactile biofeedback system to provide efficient balance biofeedback even under muscle fatigue condition. A feedback scheme based on Stevens’ power law is devised to provide 2-dimensional feedback using only four electrodes attached to the user’s leg. A pilot test involving the tracking of directions indicated by stimuli was done to select the algorithm appropriate for use in the directional perception test and the balance study. The perception, in 8 directions, of electro-tactile cues delivered using the developed scheme is compared with that of vibro-tactile cues under both normal and fatigued conditions. In addition, we have done standing balance experiments to verify the effectiveness of the developed balance biofeedback scheme. 20 healthy participants took part in these experiments that were conducted under two conditions. The perception results show that under the fatigued condition, the electro-tactile modality is more perceptible than the vibro-tactile modality. Results of the balance biofeedback experiment with no feedback, continuous stimulation with and without dead-zone and directional feedback conditions show that directional electro-tactile feedback helped the most in improving the users’ balance under normal and fatigued conditions. These promising results pave the way for future studies on the applications of this scheme for balance rehabilitation.

**INDEX TERMS** Electro-tactile feedback, biofeedback, postural control, phantom sensation, transcutaneous electrical nerve stimulation (TENS).

## I. INTRODUCTION

The number of people with age-related impairments of physical functions such as postural control is increasing with the increase in the proportion of aged populations around the world [1]. Impaired postural control adversely affects gait performance and can lead to serious injuries due to falling [2].

Many devices have been developed to aid balance training. Balance plate based systems can provide quantitative

The associate editor coordinating the review of this manuscript and approving it for publication was Lei Wei<sup>1</sup>.

balance training to users and can also be helpful for gait [3], [4]. However, such systems have limitations such as space requirement due to their bulky setup [3] or the need for a visual display to provide biofeedback [4]. To overcome these limitations, portable systems for providing balance biofeedback are being developed. A portable biofeedback system can provide sensory augmentation in various environments [5] and be applied without interfering in the subjects’ interaction with their surrounding environment [6].

The contemporary systems mostly use kinesthetic [6], [7], [8], [9], vibro-tactile [5], [10], or visual [11] modalities to

deliver feedback to the user. Kinesthetic feedback devices, such as the ones based on gyroscopes [7], or reaction wheels [8] have the advantage of assisting the user's balance by providing external force input without the need for contact with a stationary object. This feature makes such systems attractive for use in different environments. However, these systems are usually bulky [7] and cannot provide 2-dimensional feedback [7], [8]. Bechly et al. showed that directional visual biofeedback of the continuous type is more useful for balancing than the discrete one [11]. Kinesthetic feedback using haptic devices has the advantage of assisting the balance of person without disability and also stroke patients [9]. However, such devices limit hand movement since they provide cues through hand contact with the device. Recently, a device for providing 2-dimensional feedback in the form of pressing and stretching of the neck skin was developed [6]. It has a compact design and can give feedback in any direction along a 2-dimensional plane. However, it was reported to have less effect when the postural sway happens at a slow rate [6].

Currently developed vibro-tactile feedback (VTF) devices are lightweight and can provide discrete directional information in 2-dimensions [5], [10]. Furthermore, training using vibro-tactile directional biofeedback has been shown to have both short and long-term beneficial effects [12]. However, when vibro-tactile stimulation is applied directly to a muscle or tendon, it may interfere with postural control [13]. Additionally, the efficacy of VTF may be affected by reduced skin sensitivity due to muscle fatigue [14], which can easily occur during rehabilitation exercises and activities of daily life.

Electro-tactile feedback (ETF) has been reported to provide more localized sensations than VTF under normal conditions [15]. Since transcutaneous electrical nerve stimulation (TENS) generates a perceivable sensation, it may be used as a means of providing electro-tactile feedback (ETF). Furthermore, continuous stimulation with constant intensity TENS has been shown to alleviate muscle fatigue and aid in static postural control under both muscle fatigue and normal conditions [16], [17], [18]. Therefore, we hypothesized that directional ETF using TENS will be able to deliver directional information more accurately than VTF under both normal and fatigue conditions. We also hypothesized that directional ETF, due to its better perception, will improve balance in both conditions. However, existing TENS related studies have reported effects of continuous stimulation with constant intensity for postural control [16], [17], [18] and perception of directional cues rendered as different tactile stimulation sequences [15].

A tongue-mounted directional ETF device for providing biofeedback based on the center of pressure (COP) was shown to improve postural control under normal condition [19] and ankle force sensation under the fatigue condition [20]. However, this system is difficult to use in daily life due to the inconvenience of use. We recently developed a novel TENS based ETF device and showed its potential for improving static balance in the mediolateral (ML) direction

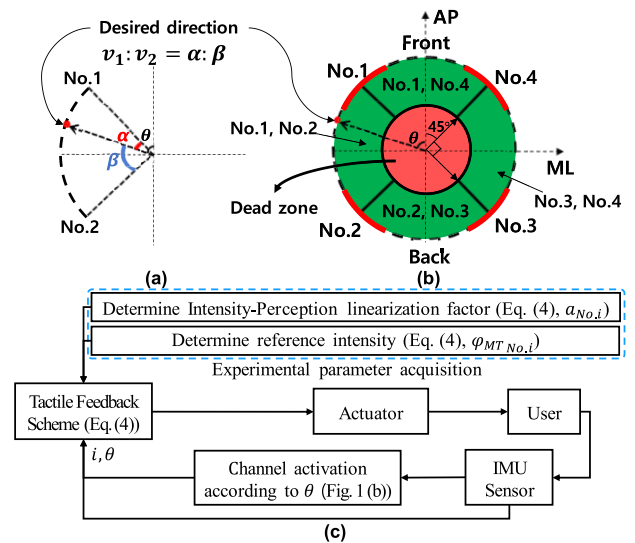


FIGURE 1. (a) The rule for determining  $v_1$  and  $v_2$  (b) The placement of the actuators and actuators activated for each direction (c) Block diagram of the tactile feedback scheme.

under muscle fatigue condition [21]. Since this was only a proof of concept, the ETF was given only in one dimension (ML) using two pairs of electrodes, and differences in the subjects' perception of each electrode pair's location were not considered.

In order to provide 2-dimensional balance feedback with the existing ETF methods, the number of electrode pairs required would be the same as the number of feedback directions [22]. Such an arrangement is impractical considering the electrode size and the minimum spacing required between electrodes. Therefore, we have proposed and evaluated a 2-dimensional electro-tactile directional feedback scheme based on Stevens' power law that utilizes four pairs of electrodes to deliver balance biofeedback under both normal and muscle fatigue conditions. The developed scheme applies Stevens' power law to reduce the differences in perception for each pair of electrodes [23]. This scheme was selected through pilot testing where we compared different algorithms. Furthermore, we have developed a prototype system to implement the proposed scheme and verified its functionality through two main studies.

In the first study, we determined the accuracy with which the ETF given in 8 directions can be perceived by the participant group and compared it with that of VTF, under both normal and fatigue conditions. In the second study, to verify the effectiveness of the developed scheme, static balance control experiments with 2-dimensional balance biofeedback delivered using the developed prototype were performed under both normal and fatigue conditions, and the participants' balance performance was analyzed. The developed scheme, the system used to test it and the pilot test are presented in Section II. The experiments performed with 20 healthy participants are presented in Section III, while their results are presented in Section IV. The results are discussed in

Section V, and the conclusions drawn from this work are presented in Section VI.

## II. BIOFEEDBACK SYSTEM DEVELOPMENT

### A. DIRECTIONAL FEEDBACK SCHEME WITH FOUR ACTUATORS

The purpose of the device control algorithm developed in this study is to deliver a phantom sensation at the point where the actuator is not attached by adjusting the intensity of the actuation. There are a number of studies that have reported control algorithms for phantom sensation using vibration [24]. D. S. Alles et al. gave a phantom sensation, which is the point on the body part, to the target position on the upper arm through linear and logarithmic control algorithm [24]. The generation of phantom sensations using electrical stimulations has been researched [25], [26], and the possibility of controlling the electro-tactile phantom sensation point has been reported. A. Pagel et al. and T. Izumi et al. showed that when electrical stimulation was applied to two adjacent areas, the point at which the stimulation was felt was different according to a simple specific ratio of the intensity at the two areas [25] or a ratio of the square of the intensity [25], [26]. However, there is a difference in the perception of stimulation at each body part [27], and the actuators used in this study are attached to four different parts. In order to generate accurately the phantom sensation between two body parts we need to consider the difference in perception of stimuli between those two parts. Therefore, we devised Steven's power law based phantom sensation generation scheme.

#### 1) STEVENS' POWER LAW APPLIED TO EACH CHANNEL

$$\Psi = k\varphi^a \quad (1)$$

$$\log(\Psi) = a \log(\varphi) + \log(k) \quad (2)$$

S. Stevens reported that the intensity of stimuli and their perception have a power relationship, which is presented in (1) [23].  $\Psi$  is the stimulus perception,  $k$  and  $a$  are constants that vary from person to person and depend on the type of stimulus and where it is being delivered, and  $\varphi$  represents the intensity of the stimulus. Equation (2) is obtained by taking the logarithm of (1). This means that perception and stimuli intensities are linear on the log scale. We use this in order to easily derive the algorithm for controlling the system. There are various phantom sensation rendering algorithms for VTF such as linear, logarithmic [24], [28], and square [28]. In order to consider the perception of each actuator attachment location, it was determined that the linear algorithm modified using (2) was most suitable for our scheme to control the phantom sensation point through modulation of the  $\Psi$  value in (2).

#### 2) PHANTOM SENSATION GENERATION SCHEME

$$\log(v \cdot \Psi) = a \log(\sqrt[a]{v} \cdot \varphi) + \log(k) \quad (3)$$

$$\varphi_{No.i} = \sqrt[a]{v_i} \cdot \varphi_{MT_{No.i}} \quad (0 \leq v \leq 1) \quad (4)$$

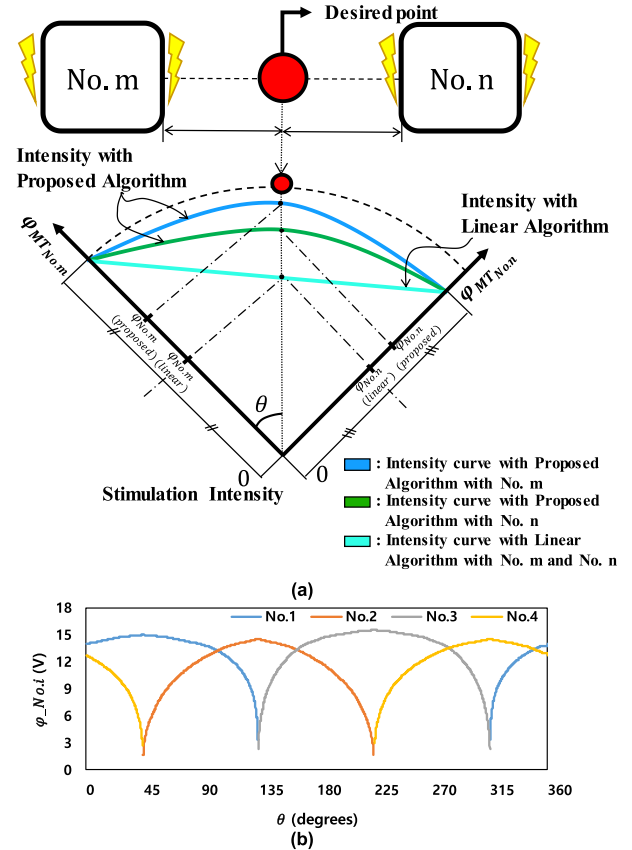


**FIGURE 2.** (a) Stimulation intensity of the proposed algorithm compared with the linear algorithm according to the desired direction. The blue and green lines indicate the intensities of the No. m and No. n actuators under the proposed algorithm. The sky-blue line indicates the intensity of both actuators according to the direction under the linear algorithm. The dash-single dotted lines ( $\varphi_{No.m}$ (proposed),  $\varphi_{No.m}$ (linear),  $\varphi_{No.n}$ (proposed),  $\varphi_{No.n}$ (linear)) indicate the intensity of each channel under the proposed and linear algorithms at the desired point (red). (b) Relationship between  $\theta$  and  $\varphi_{No.i}$  with the proposed algorithm, for a representative participant.

The purpose of this study is to generate phantom sensation by linearly adjusting the  $\Psi$  value according to the direction by varying the intensity of electro-tactile stimulation of the two actuators adjacent to the desired direction. Eq. (3) can be derived by setting the intensity  $v \cdot \Psi$  in (2). Substituting the  $\Psi$  component in (2) by  $v \cdot \Psi$ , which modifies the stimulus perception ( $\Psi$ ) so that the user's perception of stimuli at different locations can be linearized by varying the value of  $v$ . As shown in (4), the reference intensity was set as  $\varphi_{MT_{No.i}}$  to linearly adjust the  $\Psi$  value for a specific point. Stimulus intensity was modulated within a range of 0 to  $\varphi_{MT_{No.i}}$  and the resulting intensity is expressed as  $\varphi_{No.i}$  in (4), which is the input of the  $i$ th actuator where  $i$  means the index of the actuator.  $v_i$  is determined based on  $\alpha$  and  $\beta$  as shown in Figure 1(a). This means that the value of  $\Psi$  is linearly changed for each actuator placed adjacent to the phantom sensation point according to its direction, in order to indicate the directional cue through (4).  $a_{No.i}$  in (4) plays a role in changing the intensity linearly according to the user's perception. As shown in Figure 1(b), two actuators are activated

according to  $\theta$  and each actuator is positioned at 90-degree intervals. Figure 1(c) summarizes the abovementioned feedback scheme.

During experimentation, the actuators were placed around the shank near the gastrocnemius, tibialis anterior, and soleus muscles at 90-degree intervals.  $\Psi_{No_i}$  which is the perception for  $i$ th actuator is determined as  $v_i$  times  $\Psi_{MT_{No_i}}$ , where  $\Psi_{MT_{No_i}}$  is the perception for the motor threshold (MT) intensity of the  $i$ th actuator.  $\varphi_{MT_{No_i}}$  was set below the MT intensity. The motor threshold is the minimum intensity of electrical stimuli that causes muscle contraction since electrical stimulation greater than the MT results in unnecessary movement of the muscle and causes muscle fatigue [29]. If the input is controlled according to eq. (4), the directional cue can be displayed to the user while considering the perception of the part at which each actuator is attached. Figure 2(a) shows the intensity of the two stimuli according to the desired direction of the linear algorithm and the proposed algorithm through two adjacent actuators for phantom sensation generation. Figure 2(b) presents the device input values ( $\varphi_{No_i}$ ) for different values of  $\theta$  when the  $a_{No_i}$  terms are set to 6.3843, 4.0676, 4.6063, and 4.5605, and  $\varphi_{MT_{No_i}}$  are set to 14.98, 14.54, 15.53 and 14.54 V in eq. (4) for a representative participant.

### 3) PILOT TEST OF THE DEVELOPED PHANTOM SENSATION GENERATION SCHEME

The proposed phantom sensation generation scheme was compared with the logarithmic, linear, and square algorithms applied in previous studies [28]. To the best of the authors' knowledge, [30] is the only case where the vibro-tactile phantom sensation was applied to the user's calf, and they used square algorithm which is based on the energy summation model in the Pacinian channel. There is no such work reported for electro-tactile feedback. Therefore, we conducted a pilot experiment to confirm the potential of the suggested directional tactile feedback scheme. A young healthy participant participated in this experiment (Gender: Female, Age: 21 years, Height: 167 cm, Weight: 50 kg, Dominant Foot: Right). The direction indicated by the stimulus started from the right side of the participant and moved at a constant speed of 15 deg/s [30], once in the clockwise direction and once in the counter-clockwise direction, for each of the tested algorithms; logarithmic, linear, square and the proposed algorithm. The experimental parameter acquisition process carried out for the proposed algorithm with the developed VTF and ETF devices is presented in Section III-B1. The participant was asked to track the movement of the stimulus by indicating its position on the guide circle displayed on the screen (27MK400H, LG) in front of them using the mouse cursor. The participant was instructed that if the participant felt that the stimulus was cut off or they felt awkward during tracking, the participant should stop indicating the position on the screen, wait until the participant again feel the stimulus, and then start tracking again from the current perceived

TABLE 1. Results of the pilot test.

Protocol	Logarithm	Linear	Square	Power
VTF (%)	24.31±2.36	61.39±5.00	64.58±1.53	77.36±0.97
ETF (%)	13.61±4.72	48.61±15.28	68.19±2.64	80.69±7.91

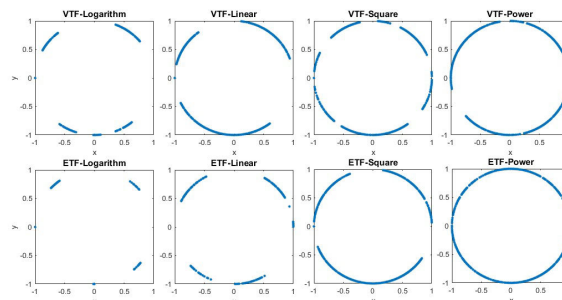


FIGURE 3. Results of the pilot test; response trace of the participant, VTF: Vibro-tactile feedback, ETF: Electro-tactile feedback, Compare proposed algorithm (power law based algorithm) with Logarithmic, Linear, Square algorithm.

position. The experiment was conducted in Logarithmic, Linear, Square, and Power sequence.

Table 1 and Figure 3 present the results of the pilot test. In Table 1, the numerical results represent the percentage of the circle traced by the participant. The participant showed a tracing accuracy of 77.36% and 80.69% with VTF and ETF, respectively, under the proposed Stevens' power law based phantom sensation generation scheme. Figure 3 presents the traces made by one participant during one trial of the pilot test. Thus, these results support the use of the power law based scheme to deliver directional feedback using phantom sensation.

### B. ELECTRO-TACTILE FEEDBACK DEVICE (ETF)

The ETF prototype used in this research is shown in Figure 4(a). To make the prototype portable, a 3D printed plate for mounting the device mainboard and components is attached on the outside of a belt with Velcro fasteners that are worn by the user around their waist. Table 2 presents the components and specifications of the ETF device. The mainboard consists of two TENS circuits to control four pairs of electrodes, an embedded controller board for generating control signals and sensing, an IMU sensor for measuring body tilt, and two DC-DC converters to modulate the supply voltage for the TENS circuits. A pair of 6 × 6 cm electrode pads (one positive and one negative) is used for actuation, and a total of four pairs are used to deliver 2-dimensional feedback. The maximum current supplied by one TENS channel (electrode pair) is 36 mA at 1 kΩ load resistance. The output signal is in the form of a train of bi-phasic asymmetrical square pulses with a frequency of 100 Hz and a width of 200 μs [20], [21]. The conventional TENS mode, which delivers high frequency and low intensity electrical pulses was used. The device latency was within 50 ms and the total weight of the system was 770 g.

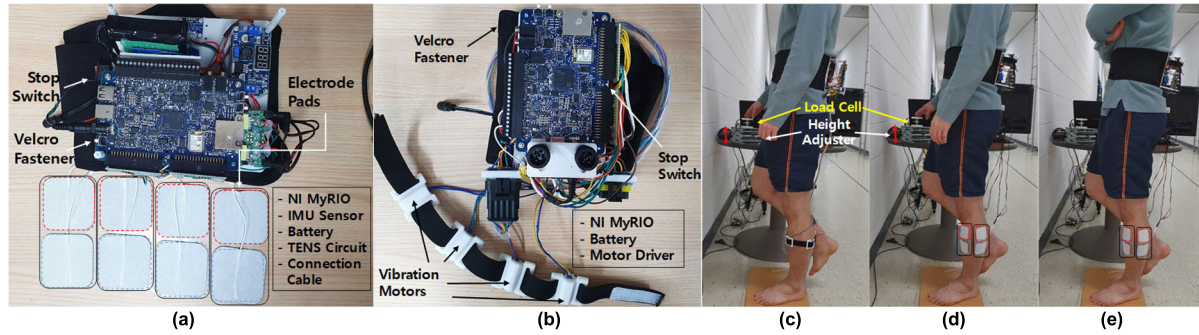


**FIGURE 4.** Developed devices (a) Electro-tactile feedback (ETF) device (b) Vibro-tactile feedback (VTF) device (c)-(e) Wearing devices and experimental set up.

**TABLE 2.** Components and specifications of the ETF device.

Specification	Value
Total Weight	770g
Delay Time	< 50ms
Output Current	0-36mA with 1000Ω
Frequency	100Hz
Pulse Width	200μs
System controller	MyRIO 1900, National Instruments®
Battery	Li-ion, DC12V/2.6Ah / 3.7V/2600mA, Coms®
IMU Sensor	9-DOF IMU, BNO-055, Bosch®
TENS Circuit	TENS-7000, Koalaty Products Inc.

**TABLE 3.** Components and specifications of the VTF device.

Specification	Value
Total Weight	780g
Frequency	300Hz
System controller	MyRIO 1900, National Instruments®
Battery	Li-ion, DC12V/2.6Ah / 3.7V/2600mA, Coms®
Vibration motor	DVM-M20, D&J®
Motor Driver	ULN2803APG, TOSHIBA

The MCU uses UDP over Wi-Fi to communicate with a laptop where software running in the LabVIEW environment (National Instruments Inc., USA) is used to send control commands and receive sensing data from the MCU. The body tilts, sensed in terms of quaternions by the IMU, are converted to roll and pitch angle values using the method described in our previous work [22]. The software embedded in the MCU operates at 100 Hz and generates control signals in the form of analog voltage for the TENS circuits according to the control commands sent by the laptop. The TENS circuits then generate TENS signals that are sent to the electrodes of the ETF device. For safety, a physical stop switch as well as a software stop button on the front panel of the LabVIEW software is provided to stop the delivery of cues at any time. The device is controlled using analog signals that can be varied with the 500-step resolution to vary the stimulus intensity between its minimum and maximum values.

**TABLE 4.** Demographic information of the participants.

Age	Height	Weight	Dominant Foot
22.3±2.8 years	167.8±7.8cm	65.8±10.9kg	20 Right

**C. VIBRO-TACTILE FEEDBACK DEVICE (VTF)**

The VTF device, developed to compare the accuracy of perception for directional cues with the ETF device, is shown in Figure 4(b). Table 3 presents the components and specifications of the VTF device. It consists of four vibration motors, an embedded controller board (MCU) for managing the communication and control, a motor driver to interface the vibration motors with the MCU, a DC-DC converter to modulate the voltage for the motor driver, a battery pack, and a power switch. The frequency of the vibration motors is about 300 Hz. The weight of the VTF device is 780 g. The vibration motors are housed in 3D-printed plastic structures threaded onto an elastic band with Velcro fasteners for easy donning and doffing.

The operation method of the VTF device is similar to the ETF system. To maintain consistency, the duty cycle of the pulse width modulation (PWM) signals sent to the motor driver by the MCU to control the vibration motors is also varied with 500-step resolution. Similar to the ETF device, the laptop and MCU of the VTF device also interact using UDP communication over Wi-Fi and its control software also runs in the LabVIEW environment.

**III. EXPERIMENTS**

**A. PARTICIPANTS**

We conducted perception and balancing experiments with and without muscle fatigue to verify the effectiveness of the developed scheme. 20 healthy young people (10 male, 10 female) participated in this experiment. Table 4 shows the demographic information of the participants. None of the participants suffered from any neurological or musculoskeletal disorders, and none of them had any issues with respect to localized muscle fatigue generation, unilateral standing, and use of the ETF and VTF devices in the study. This study was conducted in accordance with the Declaration of

Helsinki, and was approved by the Institutional Review Board of Gwangju Institute of Science and Technology, Gwangju, South Korea (20210609-HR-61-07-04). All participants gave written informed consent before participation in the study.

**B. PROTOCOL**

We carried out two experiments in this study. One was a directional perception test to determine the perceptibility of directed stimuli delivered using the developed directional feedback scheme. The other was a balance study to determine the efficacy of the balance biofeedback delivered by the developed scheme. Before starting the experiments, we conducted an experimental parameter acquisition process to acquire the parameters needed to tune the system in order to deliver the directional feedback.

The experiments were carried out under both normal and fatigued conditions over a course of two consecutive days; one day for normal condition tests and one for fatigued condition tests. For the trials under muscle fatigue condition, the participants induced fatigue in their leg muscles by standing in a bipedal stance and repeatedly lifting and lowering their heels to the point of failure [23]. This exercise was performed before the start of the directional perception test and before the start of each protocol of the balance study [23]. Before the experiments under the normal condition, the participants rested to remove any tiredness or fatigue. The normal condition experiment was started when the participant determined that their condition was similar to that before the start of the fatigue generation process of the fatigue experiment.

The order of the experimental conditions was randomized. It was ensured that the participants did not have any leg muscle fatigue prior to the start of trials on both experiment days. Prior to the commencement of each set of experiments, the experimental protocol and equipment used in the experiment were explained to the participants.

**1) EXPERIMENTAL PARAMETER ACQUISITION**

Once the actuators were placed at the locations described above, a simple test (Experimental parameter acquisition process, See Figure 1(c)) was conducted to obtain the  $a_{No,i}$ ,  $\varphi_{No,i}$  and  $\varphi_{MT_{No,i}}$  values used in eq. (4) for each actuator of both devices (ETF and VTF). For the ETF, the MT was determined by having the participant sit in a relaxed posture, and gradually increasing the intensity of the signal delivered by each electrode pair. The intensity at which observable muscle contraction occurred was considered as the MT [18]. And it is the ‘Determine reference intensity’ process in Figure 1(c).

In order to determine the stimulus sensitivity, i.e. the minimum change in stimulus intensity that can be perceived by the participant at a given location, a method based on the ascending method of limit, which is described in [15], was used. It is the ‘Determine Intensity-Perception linearization factor’ in Figure 1(c). The participants stood in a bipedal stance with their finger continuously placed on a button, and the stimulation intensity was increased gradually, starting at 0 intensity. The participant was asked to press the button when

**TABLE 5. Experimental protocol for the balance study.**

Trial	Conditions
NF	No Feedback
CS	Continuous Stimulation
CSD	Continuous Stimulation with Dead zone
DF	Directed Feedback

they felt the stimulation get stronger. When the button was pressed with a force of 2N, a beep sound was produced and we stopped increasing the intensity. The participant was then asked to consider the current intensity as the starting point and to press the button again when they felt a change in the intensity, and we again increased the intensity gradually. The log of the average of the two intensity values thus obtained was considered as the y value for the first order polyfit function built-in MATLAB®. This process was repeated until the MT value was reached, and the log of the number of the process iteration was used as the x value for the polyfit function. The  $a_{No,i}$  value output of this function thus obtained was then used in eq. (4). Before starting the experiment, the maximum intensity value of each device, which is  $\varphi_{MT_{No,i}}$ , was tuned so that the four actuators’ perceived intensities were the same according to the participant’s perception. Since the devices weigh almost the same, it is expected that their weight related effects on the participants’ balance will be the same. For the VTF device, the actuators were attached in the same locations as the ETF actuators. The maximum stimulation value was set as PWM duty equal to 1, i.e. the maximum output of the vibration motor. The entire experimental parameter acquisition process took less than 15 minutes.

**2) DIRECTIONAL PERCEPTION TEST**

As shown in Figure 4(c) and (d), during the directional perception test trials, the participants stood on their non-dominant leg [6], placed their fingers on a plate to gain light-touch support, and looked straight at a wall to minimize visual disturbance. The light-touch support gained through the hand helps the participants in maintaining the one-leg stance, thus allowing them to focus on the stimuli being provided to them. In order to prevent the participant from gaining too much support, a load cell was attached under the support plate and a warning sound was generated when a force of 2 N or more was applied to it [24].

To determine the directional perception of the actual (at actuator location) and phantom (between actuator locations) sensations, stimuli in 8 different directions; right (R), right forward (RF), forward (F), left forward (LF), left (L), left backward (LB), backward (B) and right backward (RB), were applied in random order with each direction being applied twice during each trial. To do this, the value of  $\theta$  was varied with intervals of 45 degrees from 0 to 360 degrees according to the desired stimulation direction. The average circumference of an adult’s shank is 35-36 cm [25], and the average two-point discrimination threshold for electro-tactile stimuli

is 3-4cm [26]. Therefore, in this study, the average distance between the midpoints of the actuators was kept at about 9 cm. Each directional cue was provided for 6 seconds and there was a gap of 4 seconds between cues. This gave the participants a total of 10 seconds to determine the direction of the cue and communicate it verbally to the experimenter [27].

This protocol was done two times each for both the devices (ETF and VTF). In order to match the experimental conditions of the perception and balance studies, the participants adopted the same posture and wore the belt containing the device motherboard around their waist in both studies.

### 3) BALANCE STUDY

Before the start of this set of trials, the participants performed familiarization with the directed balance biofeedback while standing in a bipedal stance. In each trial, the participants tried to maintain their balance while standing in the one-leg stance for 30 seconds on a hard, flat plate with their eyes open and looking straight at a wall. As shown in Figure 4(e) in the balance trials, the participants stood on their non-dominant leg, crossed their arms across their chest, and raised their dominant foot clear off the ground [6]. The participants assumed the posture before starting each trial, and when the posture was stabilized, the system was calibrated to set the zero reference for the trunk tilt angle measurement [6].

The four stimulation/feedback conditions shown in Table 5 were tested under both normal and fatigue conditions. For consistency, participants wore the complete device in all the trials. In the no feedback (NF) condition, participants received no electrical stimulation. In the continuous stimulation (CS) condition, the participants received continuous electrical stimulation with an intensity just below the motor threshold ( $\varphi_{MT_{No_i}}$ ) for the entire duration of the trial at all the actuator locations. A dead zone representing 1-degree tilt in all directions [5] was set up as shown in Figure 1(b). In the continuous stimulation with dead zone (CSD) protocol, the participant received electrical stimulation at all actuator locations with  $\varphi_{MT_{No_i}}$  intensity when the sum of the squares of their mediolateral (ML) and anteroposterior (AP) trunk tilts exceeded the dead zone [5]. In the directed feedback (DF) protocol, when the participant's trunk tilt exceeded the dead zone, electrical stimulation was delivered to them according to the tilt direction. This is done by setting the value of  $\theta$  according to the direction of the trunk tilt. The dead zone is applied in the DF mode to avoid any confusion about the zero tilt position of the trunk [6]. The application of a dead zone may itself affect postural control. The existing research on the application of TENS for postural control has utilized only continuous stimulation with constant intensity, without the application of a dead zone. Therefore, the CSD mode has been added in this study to check the effects of the application of a dead zone on postural control.

### C. DATA ANALYSIS

During the directional perception test, the actual directions of the given cues and the participants' answers were recorded

TABLE 6. Meanings of the abbreviations.

Parameter	Meaning
VTF	Vibro-Tactile Feedback
ETF	Electro-Tactile Feedback
NF	No Feedback
CS	Continuous Stimulation
CSD	Continuous Stimulation with Dead zone
DF	Directed Feedback
MVD	Mean Velocity Displacement
PD	Planar Deviation
RMS of ML	Root Mean Square of Mediolateral trunk tilt
RMS of AP	Root Mean Square of Anteroposterior trunk tilt

during all trials. During the balance study, the trunk tilt data for both ML and AP directions, measured using the IMU, was stored in the laptop at 100Hz. Data from the middle 25-seconds of the measured 30 seconds were used for analysis [6]. Data from all the participants were included in the post-experiment analysis, which was done in a blinded manner.

From the collected data, projections of trunk tilt in ML and AP directions ( $PT_{ML}$  and  $PT_{AP}$ ) were calculated by multiplying the height of the IMU sensor from the ground with the trunk tilt angles in the ML and AP directions ( $TrunkTilt_{ML}$  and  $TrunkTilt_{AP}$ ), respectively. The PT values thus calculated were used to calculate the planar deviation (PD) and mean velocity displacement (MVD) of the trunk movements. In addition, the root mean square (RMS) values of  $TrunkTilt_{ML}$  and  $TrunkTilt_{AP}$  were also calculated. These parameters are commonly used as indicators of the quality of balance [6], [9], [28].

$$MVD (cm/s) = \frac{\sum_{i=0}^N \sqrt{\frac{(PT_{ML}(i+1)-PT_{ML}(i))^2 + (PT_{AP}(i+1)-PT_{AP}(i))^2}{t_{i+1}-t_i}}}{N} \quad (5)$$

$$PD (cm) = \sqrt{\sigma^2 PT_{ML} + \sigma^2 PT_{AP}} \quad (6)$$

$$RMS \text{ of ML} = \sqrt{\frac{\sum_{i=0}^N TrunkTilt_{ML}^2}{N}} \quad (7)$$

$$RMS \text{ of AP} = \sqrt{\frac{\sum_{i=0}^N TrunkTilt_{AP}^2}{N}} \quad (8)$$

MVD is the average of the PT speeds in the ML and AP directions. PD is the square root of the sum of the squares of the variance of PT in the ML and AP directions. This indicates how spread out the PT is. RMS values of ML and AP tilts indicate how far the trunk tilt angle deviates from the zero point in each direction. For all these parameters, higher values

**TABLE 7. Outcomes of the directional perception test.**

Parameter	VTF	ETF
Accuracy (Normal, %)	90.47±10.53	93.91±5.97
Accuracy (Fatigue, %)	83.28±9.23	91.25±6.45

mean a higher level of balance difficulties, resulting in lower quality of balance [6], [9].

A two-way repeated measures analysis of variance (RMANOVA) was used to investigate the difference due to Condition (Normal, Fatigue) and Device (Vibro-tactile feedback, Electro-tactile feedback) in the accuracy of perception of the directed cues. In addition, two-way RMANOVA was used to analyze the differences due to Condition (Normal, Fatigue) and Feedback (NF, CS, CSD, DF) in MVD, PD, and RMS of ML and AP tilts. The Q-Q plot evaluation tool was utilized to observe the distribution of data, which was found to be within the acceptable range of normal distribution. Mauchly’s test of Sphericity was used to confirm the validity of the RMANOVA results ( $p < .05$ ) and Greenhouse Geisser corrections (for  $\epsilon < .75$ ) were applied where sphericity was violated. Post hoc tests were conducted with the application of Bonferroni correction. Partial eta squared ( $\eta_p^2$ ) was calculated as a measure of the effect size for two-way RMANOVA. All statistical analyses were performed using SPSS V20.0 (IBM Corp., USA).

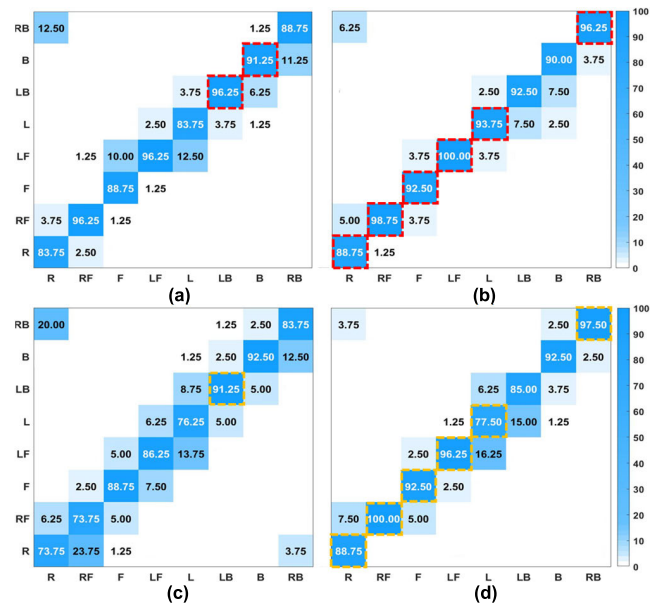
**IV. RESULTS**

Table 6 lists the full forms of the abbreviations used in the post-experiment analysis. Table 7 and 8 present the mean and standard deviations (SD) of the overall outcomes of directional perception test and balance study, respectively.

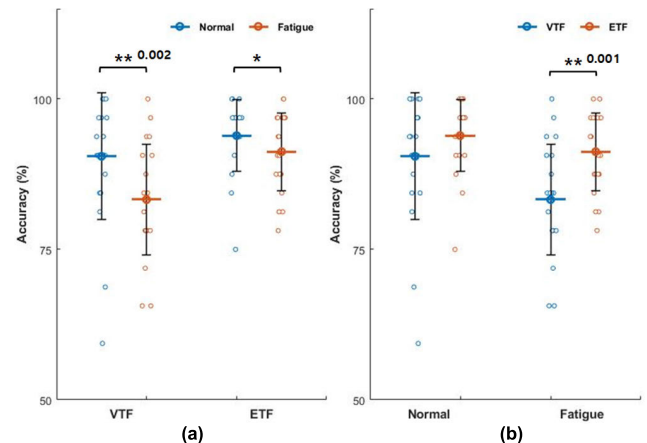
**A. DIRECTIONAL PERCEPTION TEST (TWO-WAY RMANOVA)**

Table 9 presents the mean and SD of the  $\varphi_{MTNoi}$  and  $a$  values, which were obtained from the experimental parameter acquisition process included in these experiments with the VTF and ETF. The confusion matrices of mean accuracy for each direction of VTF and ETF with each condition are shown in Figure 5. Higher accuracy for each direction is highlighted with dotted boxes under normal (between Figure 5(a) and (b)) and fatigue conditions (between Figure 5(c) and (d)). It can be seen that all the incorrect directions reported in these trials were adjacent to the correct directions.

As shown in Figure 5(a) and (b), apart from the LB and B directions, the directional cues delivered in all other directions using ETF under normal condition had greater perceptibility than those delivered using VTF. The muscle fatigue condition reduced the perceptibility of VTF cues. Under normal condition, the perceptibility for only four directions was below 90% (see Figure 5(a)). Whereas, under fatigue condition, perceptibility for six directions fell below 90% with three of them being below 80% (see Figure 5(c)). The perceptibility of ETF cues was also reduced due to fatigue,



**FIGURE 5. Results of the directional perception test; confusion matrices of the direction perception mean accuracy for both devices. x-axis is the actual answer and y-axis is the answer selected by the participant. Red and yellow dotted boxes indicate higher accuracy in each direction between VTF and ETF under normal and fatigue conditions, respectively. (a) VTF under normal condition (b) ETF under normal condition (c) VTF under fatigue condition, and (d) ETF under fatigue condition.**



**FIGURE 6. The scatter plot with mean, SD, and two-way RMANOVA results for the overall accuracy recorded during the directional perception test. (a) Comparison of the condition (Normal, Fatigue). (b) Comparison of the modality (VTF, ETF). Statistically significant differences are marked based on the Post-hoc pairwise comparisons (\*:  $p < 0.05$ , \*\*:  $p < 0.01$  \*\*\*:  $p < 0.001$ ). The scatter plots show the data of each of the participants. The colored bars show the mean and the error bars show the standard deviation.**

but it remained substantially higher than that of VTF cues under the same condition. For six out of the eight directions tested ETF showed greater perceptibility than VTF under the fatigue condition, and it was only lesser than VTF for the LB directed cues (see Figure 5(c) and (d)).

An interesting observation with ETF under normal and fatigue conditions (Figure 5(b) and (d)) was that under the normal condition the perceptibility for R directed cues was



**TABLE 8. Outcomes of the directional perception test.**

Condition Parameter	Normal				Fatigue			
	NF	CS	CSD	DF	NF	CS	CSD	DF
MVD (cm/s)	2.02±0.56	2.10±0.65	2.44±0.76	2.10±0.60	2.97±1.55	2.85±1.27	3.41±1.41	2.45±0.87
PD (cm)	1.24±0.39	1.23±0.45	1.33±0.55	0.98±0.20	1.78±0.88	1.59±1.01	1.81±1.01	1.15±0.36
RMS of ML (degrees)	0.80±0.38	0.76±0.36	0.67±0.26	0.47±0.14	1.13±0.65	0.98±0.59	0.83±0.45	0.50±0.24
RMS of AP (degrees)	0.86±0.33	0.87±0.39	0.77±0.35	0.52±0.08	1.21±0.45	1.03±0.75	0.85±0.41	0.56±0.13

**TABLE 9. Experimental parameters of 20 participants obtained from the Directional perception test and the balance study.**

Parameter	Values			
	No.1	No.2	No.3	No.4
$\varphi_{MTNoi}$ (VTF) (PWM duty)	0.989±0.023	0.994±0.018	0.99±0.021	0.976±0.03
$a$ (VTF)	1.44±0.20	1.41±0.22	1.46±0.22	1.52±0.25
$\varphi_{MTNoi}$ (ETF) (V)	14.84±0.397	14.34±0.502	14.06±0.784	13.86±1.01
$a$ (ETF)	5.59±0.97	5.92±1.11	5.88±0.92	5.96±0.82

**TABLE 10. Results of the 2-way RMANOVA.**

Parameter	Factor	F	P-value	$\eta_p^2$
Accuracy	Condition	(1, 19) = 17.574	< .001	.481
	Device	(1, 19) = 9.916	< .01	.343
	Interaction	(1, 19) = 4.674	< .05	.197
MVD	Condition	(1, 19) = 13.182	< .01	.410
	Feedback	(3, 57) = 8.427	< .001	.307
	Interaction	(3, 57) = 2.584	.062	.120
PD	Condition	(1, 19) = 8.113	< .05	.299
	Feedback	(3, 57) = 7.248	< .001	.276
	Interaction	(3, 57) = .996	.401	.050
RMS of ML tilt	Condition	(1, 19) = 4.654	< .05	.197
	Feedback	(3, 57) = 14.124	< .001	.426
	Interaction	(3, 57) = 2.334	.084	.109
RMS of AP tilt	Condition	(1, 19) = 3.150	.092	.142
	Feedback	(3, 57) = 14.944	< .001	.440
	Interaction	(2, 38.008) = 1.548	.226	.075

the lowest whereas under the fatigue condition that for the L direction was the lowest. This may be attributed to the greater muscle mass on the left side of the left leg, which may result in greater effect of muscle fatigue on skin sensation in this area [29]. The overall perception results show that the directed feedback generated by our proposed algorithm has greater perceptibility when it is delivered via ETF as compared to VTF, thus making it more suitable for ETF based application.

Results of the two-way RMANOVA of the accuracy for all directions carried out to study the effects of condition (normal, fatigue) and device (VTF, ETF), are presented in Table 10. Simple main effects were tested for post-hoc analysis, due to the significant interaction of condition and device on accuracy. The results of the post-hoc tests are presented in Figure 6. Perception accuracy of both devices decreased significantly under the fatigue condition (VTF:  $P < .01$ , Cohen's

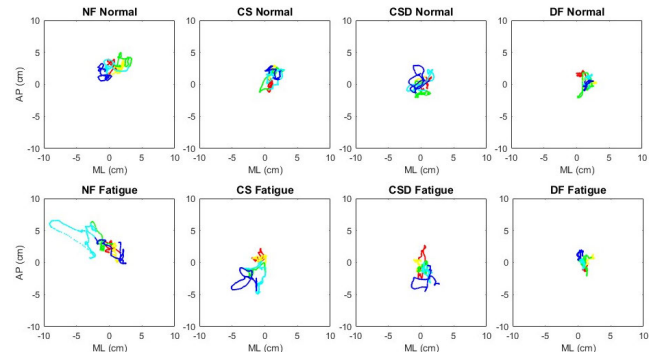


**FIGURE 7. The stabilograms (Projection of ML, AP trunk tilt) of one participant during all trials. In each figure, the first column is the normal condition and the second column is the fatigue condition. Red to blue color transition represents trial time from start to end.**

$d = 1.03$ , ETF:  $P < .05$ , Cohen's  $d = 0.60$ ). However, the perception accuracy of ETF cues was significantly higher than that of VTF cues in the fatigue condition ( $P < .01$ , Cohen's  $d = 1.42$ ).

**B. BALANCE STUDY (TWO-WAY RMANOVA)**

Stabilograms showing the ML and AP trunk tilts of one healthy participant under all the trial conditions are shown in Figure 7. It can be observed that the DF trial condition results in a more congested stabilogram, which indicates better balance control [6]. Results of the two-way RMANOVA of MVD, PD, RMS of ML and AP tilt, carried out to investigate the effects of condition (normal, fatigue) and feedback (NF, CS, CSD, DF) are presented in Table 10. For MVD, PD, RMS of ML and AP tilt, no significant interaction led to post-hoc analysis of condition and feedback separately. The results of all these post-hoc tests are presented in Figure 8 and Figure 9.

As shown in Figure 8(a)-(d), use of DF resulted in no significant difference in MVD as compared to NF, however PD (Normal:  $P < .05$ , Cohen's  $d = 1.19$ , Fatigue:  $P < .05$ , Cohen's  $d = 1.32$ ), RMS of ML (Normal:  $P < .01$ , Cohen's  $d = 1.63$ , Fatigue:  $P < .01$ , Cohen's  $d = 1.82$ ) and AP tilt (Normal:  $P < .01$ , Cohen's  $d = 2.00$ , Fatigue:  $P < .001$ , Cohen's  $d = 2.78$ ) showed significant reductions under both normal and fatigue conditions. Whereas, CS did not result in any significant difference in the balance measures as compared to NF. Furthermore, Figure 8(a) and (d) show that, under the normal condition, MVD under CSD was significantly greater than that under NF ( $P < .05$ , Cohen's  $d = 0.89$ ), and under the

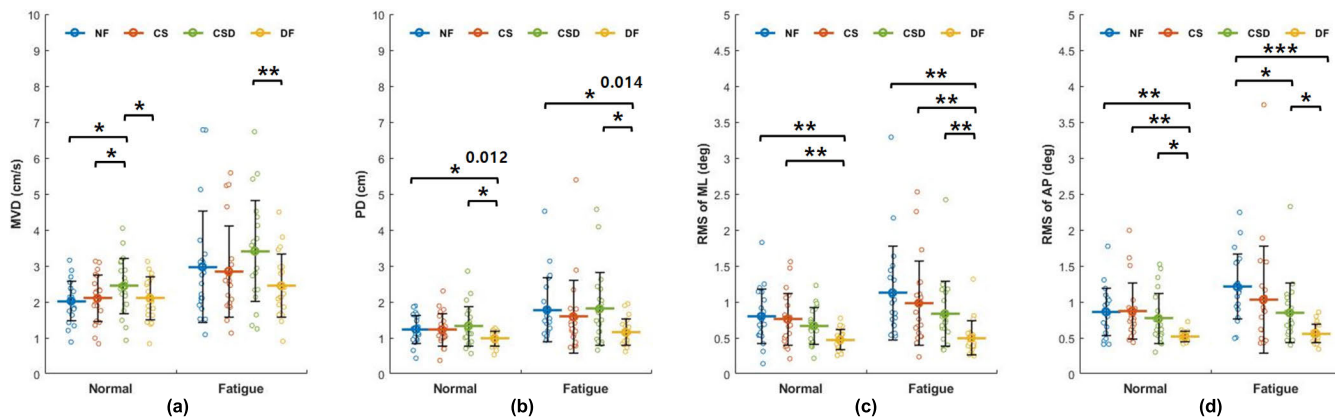


**FIGURE 8.** The scatter plot with mean, SD, and two-way RMANOVA results for the balance experiment. Comparison of feedback types (NF, CS, CSD, DF) under each of the test conditions (a) MVD (b) PD (c) RMS of ML, and (d) RMS of AP. Statistically significant differences are marked based on the Post-hoc pairwise comparisons (\*:  $p < 0.05$ , \*\*:  $p < 0.01$  \*\*\*:  $p < 0.001$ ). The scatter plots show data of each of the participants. The colored bars show the mean and the error bars show the standard deviation.

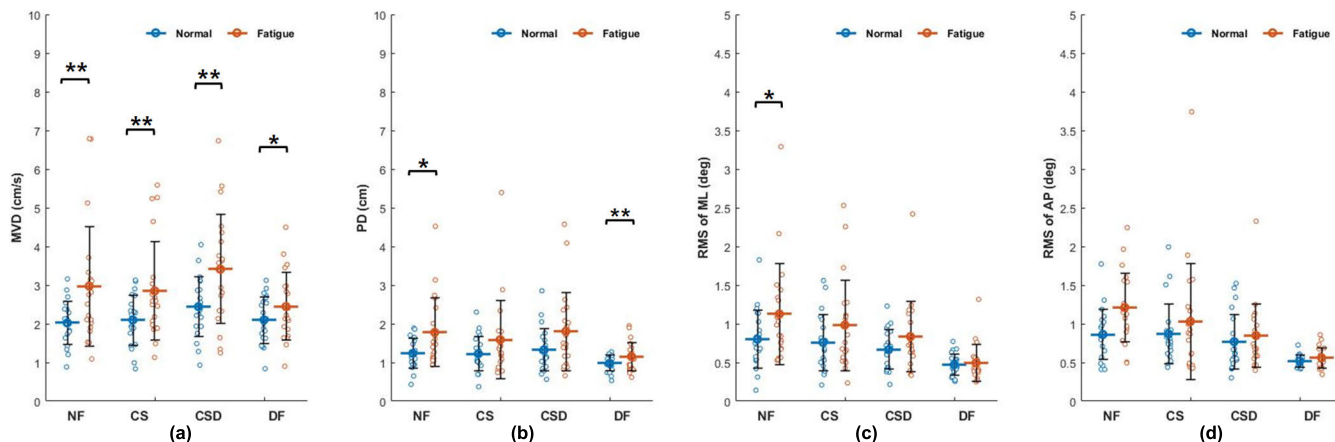


**FIGURE 9.** The scatter plot with mean, SD, and two-way RMANOVA results for the balance experiment. Comparison of test conditions (Normal, Fatigue) under each type of feedback (a) MVD (b) PD (c) RMS of ML, and (d) RMS of AP. Statistically significant differences are marked based on the Post-hoc pairwise comparisons (\*:  $p < 0.05$ , \*\*:  $p < 0.01$  \*\*\*:  $p < 0.001$ ). The scatter plots show the data of each of the participants. The colored bars show the mean and the error bars show the standard deviation.

fatigue condition, RMS of AP under CSD was significantly less than that under NF ( $P < .05$ , Cohen's  $d = 1.18$ ). This indicates that the proposed directed feedback (DF) is effective in reducing the tilt angle and the amount of movement in both ML and AP directions.

As shown in Figure 9(a)-(d), under the NF with fatigue condition, there was significant increase in MVD ( $P < .01$ , Cohen's  $d = 1.15$ ), PD ( $P < .05$ , Cohen's  $d = 1.12$ ) and RMS of ML ( $P < .05$ , Cohen's  $d = 0.88$ ), as compared to the normal condition. This indicates that muscle fatigue makes it difficult to maintain balance.

**V. DISCUSSION**

In this work, we proposed a scheme for delivering TENS based electro-tactile biofeedback to the lower limb that can be used even under muscle fatigue conditions with high perception accuracy. Furthermore, we developed a prototype system to implement the scheme and performed directional perception tests and a balance study to verify its functionality.

**A. DIRECTIONAL PERCEPTION TEST**

According to Han et al., artificially induced local muscle fatigue reduces skin sensation in the affected area, and this was verified in the bicep and rectus femoris areas through experiments [29]. Similarly, in our experiments, repeated plantar flexion to induce muscle fatigue reduced the skin sensitivity near the actuator locations, which resulted in the decreased accuracy of perception for both the tested modalities. However, the fatigue condition caused the ETF modality ( $P < .05$ , Cohen's  $d = 0.60$ ) to have a less significant decrease in perception accuracy than the VTF modality ( $P < .01$ , Cohen's  $d = 1.03$ ), as compared to the normal condition (See Figure 6(a)). Furthermore, the perception accuracy of the ETF modality was significantly higher than that of the VTF modality under the fatigue condition ( $P < .01$ , Cohen's  $d = 1.42$ , See Figure 6(b)). According to Han et al., muscle fatigue delays the information transfer in the intracutaneous somatosensory system, which causes an increase in the perception errors [29]. However, since TENS can increase

somatosensory input and alleviate muscle fatigue [20], [30], perception accuracy showed a lesser decrease with TENS based feedback. On the other hand, there was no significant difference between devices (VTF vs ETF) under the normal condition (See Figure 6(b)). D. Stanke et al. showed that ETF modality has a more localized sensation than VTF when cues are delivered to the finger in the form of electrode switching, where two out of four electrodes placed around the finger are switched to represent a cue direction [31]. Their scheme required a temporal separation between stimuli to convey the directional information to the user. Whereas, our developed scheme utilizes the intensity difference between pairs of actuators to give a single directed cue, which enables our system to continuously give directional feedback to the user.

Thus, the results of the directional perception test show that, especially under the fatigue condition, the ETF modality is more perceptible than VTF when 4 actuators are used to generate directional cues in 8 directions. Similar to the observations reported in [27], most of the participants felt that the intensity of electrical stimulation in all directions was the same, even though there was a considerable difference in sensitivity between locations. The high perceptibility of ETF under both normal and fatigue conditions also indicates that it has the potential for greater efficacy as a biofeedback modality used under both these conditions.

## B. BALANCE STUDY

Previous research showed that continuous stimulation using TENS improved balance during one-leg stance under the normal condition [32], [33], [34]. Delivery of constant sensory threshold intensity stimulation at the gastrocnemius using two pairs of electrodes significantly reduced the body sway velocity [32]. In addition, electrical stimulation below sensory threshold intensity delivered to the tibialis anterior muscle using one channel improved balance in the AP direction [33]. However, Cho et al. reported that stimulation with an intensity equal to 2-3 times the sensory threshold delivered using two channels more significantly improved body sway length and velocity than the sensory threshold stimulation during single leg stance under the fatigue condition [20]. Thus, we expected that the just below motor threshold intensity stimulation applied using four channels (CS) would help improve balance more in the fatigue condition than in the normal condition however, this did not happen in our study (See Figure 8(a)-(d)). Muscle fatigue makes it difficult to balance in the single leg stance, which mainly results in increased ML sway [23]. Similarly, the MVD, PD, and RMS of ML showed significant increases in the NF under fatigue condition, as compared to NF under normal condition (See Figure 9(a)-(d)). In contrast, CS under fatigue condition showed a significant increase only in MVD ( $P < 0.01$ , Cohen's  $d = 1.05$ ). This indicates that when continuous stimulation is provided to the participant, only the amount of movement done for balancing increases due to fatigue, while the radius of movement remains unchanged. Thus, in contrast to the NF

condition, the provision of CS through four pairs of electrodes mitigated the deterioration of balance due to muscle fatigue.

The improvement in all balance measures, except MVD, with DF under both conditions (See Figure 8(a)-(d)) indicates that the provision of directed feedback helped the participant in improving their posture. In addition, as shown in Figure 9(a), (c), and (d) the significance of the difference between the normal condition and the fatigue condition is less than that of other feedback conditions for MVD and there is no difference between the normal condition and the fatigue condition in the RMS of ML and AP. Thus, in contrast to the NF condition, the DF condition appears to alleviate the fatigue condition. However, in Figure 9(b), the PD values for the DF trial show a significant difference, this is thought to be because of the reduction in the range of trunk tilts of the participant in the normal condition, which was more than that in the fatigue condition (See Figure 8(b)).

Under the normal condition, MVD under CSD was significantly increased compared to that under NF ( $P < 0.05$ , Cohen's  $d = 0.89$ , Figure 8(a)). It is thought that although the non-directional constant electrical stimulation with the dead zone informed the participants that their body sway was greater than the dead zone, it did not provide any information about the direction, which resulted in the increased amount of body sway. However, as shown in Figure 8(b)-(d), as compared to NF, the trunk tilt did not increase, and similar to the CS condition, there was no difference between the normal condition and the fatigue condition in all parameters except the MVD. In addition, there is no significant difference between CS and CSD, apart from the MVD parameter under the normal condition, which is increased. The only difference between CS and CSD trials is the dead zone, and the results show that the application of the dead zone did not have any additional effect on the participants' balance. However, when the presence of a dead zone is combined with directed ETF, as in the DF condition, the participants' balance is significantly improved, especially under the muscle fatigue condition.

Thus, the developed feedback scheme can provide 2-dimensional feedback under normal and muscle fatigue conditions. However, further in-depth studies are required to characterize fully the feedback generated by this method and to refine further the method itself. Furthermore, Afzal et al. showed that proportionally increasing the intensity of VTF according to movement error significantly improved the gait symmetry of stroke survivors [35]. Additionally, in our previous exploratory study on TENS-based biofeedback, where the intensity of the stimulation provided to the medial and lateral gastrocnemius muscles using two pairs of electrodes varied according to the ML trunk tilt, improved the trunk tilt of healthy participants during one-leg stance under the fatigue condition [21]. Building upon these previous observations and the directional feedback related results of the current study, in future research, we intend to find an optimal electro-tactile feedback scheme that combines intensity encoding and directional information to help improve

the standing and gait balance of patients such as stroke survivors.

## VI. CONCLUSION

In this study, we proposed an electro-tactile balance biofeedback scheme that utilizes Stevens' power law to deliver TENS based 2-dimensional cues to the leg. The effectiveness of this scheme was demonstrated through an experiment with 20 young healthy participants. Experimental results show that directional cues delivered using the proposed scheme can be perceived more accurately than those delivered using the vibro-tactile modality under fatigue condition. Furthermore, directional balance biofeedback delivered using the proposed scheme helps in improving the user's balance under both normal and fatigue conditions. This study also revealed that continuous application of electrical stimulation through the four pairs of electrodes below the motor threshold appears to have no significant effect on balance as compared to a no stimulation condition. However, it may mitigate the effects of muscle fatigue. Thus, the developed TENS based 2-dimensional ETF scheme and the prototype implementing it have the potential to improve balance during gait and activities of daily life.

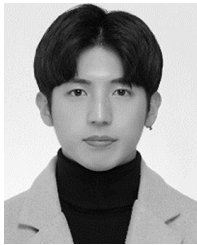
## ACKNOWLEDGMENT

(Junyeong Lee and Hosu Lee contributed equally to this work.)

## REFERENCES

- N. D. Carter, P. Kannus, and K. Khan, "Exercise in the prevention of falls in older people," *Sports Med.*, vol. 31, no. 6, pp. 427–438, 2001.
- N. B. Alexander, "Postural control in older adults," *J. Amer. Geriatrics Soc.*, vol. 42, no. 1, pp. 93–108, Jan. 1994.
- F. A. Siddiqi and T. Masood, "Training on Biodex balance system improves balance and mobility in the elderly," *JPMA. J. Pakistan Med. Assoc.*, vol. 68, no. 11, pp. 1655–1659, 2018.
- P. V. Mhatre, I. Vilares, S. M. Stibb, M. V. Albert, L. Pickering, C. M. Marciniak, K. Kording, and S. Toledo, "Wii fit balance board playing improves balance and gait in Parkinson disease," *PM&R*, vol. 5, no. 9, pp. 769–777, Sep. 2013.
- C. Wall, D. M. Wrisley, and K. D. Statler, "Vibrotactile tilt feedback improves dynamic gait index: A fall risk indicator in older adults," *Gait Posture*, vol. 30, no. 1, pp. 16–21, Jul. 2009.
- H. Lee, A. Eizad, J. Park, Y. Kim, S. Hwang, M.-K. Oh, and J. Yoon, "Development of a novel 2-dimensional neck haptic device for gait balance training," *IEEE Robot. Autom. Lett.*, vol. 7, no. 2, pp. 2511–2518, Apr. 2022.
- D. Lemus, A. Berry, S. Jabeen, C. Jayaraman, K. Hohl, F. C. T. van der Helm, A. Jayaraman, and H. Vallery, "Controller synthesis and clinical exploration of wearable gyroscopic actuators to support human balance," *Sci. Rep.*, vol. 10, no. 1, pp. 1–15, Jun. 2020.
- M. R. Afzal, A. Eizad, C. E. Palo Peña, and J. Yoon, "Evaluating the effects of kinesthetic biofeedback delivered using reaction wheels on standing balance," *J. Healthcare Eng.*, vol. 2018, pp. 1–10, Jun. 2018.
- M. R. Afzal, H.-Y. Byun, M.-K. Oh, and J. Yoon, "Effects of kinesthetic haptic feedback on standing stability of young healthy subjects and stroke patients," *J. Neuroeng. Rehabil.*, vol. 12, no. 1, pp. 1–11, Dec. 2015.
- K. H. Sienko, M. D. Balkwill, L. I. E. Oddsson, and C. Wall, "Effects of multi-directional vibrotactile feedback on vestibular-deficient postural performance during continuous multi-directional support surface perturbations," *J. Vestibular Res.*, vol. 18, nos. 5–6, pp. 273–285, 2008.
- K. E. Bechly, W. J. Carender, J. D. Myles, and K. H. Sienko, "Determining the preferred modality for real-time biofeedback during balance training," *Gait Posture*, vol. 37, no. 3, pp. 391–396, Mar. 2013.
- D. S. Alles, "Information transmission by phantom sensations," *IEEE Trans. Man-Machine Syst.*, vol. MMS-11, no. 1, pp. 85–91, Mar. 1970.
- T. Izumi, N. Hoshimiya, A. Fujii, and Y. Handa, "A presentation method of a traveling image for the sensory feedback for control of the paralyzed upper extremity," *Syst. Comput. Jpn.*, vol. 19, no. 8, pp. 87–96, Aug. 1988.
- A. Pagel, A. H. Arieta, R. Riener, and H. Vallery, "Effects of sensory augmentation on postural control and gait symmetry of transfemoral amputees: A case description," *Med. Biol. Eng. Comput.*, vol. 54, no. 10, pp. 1579–1589, Oct. 2016.
- G. A. Gescheider, *Psychophysics: The Fundamentals*. London, U.K.: Psychology Press, 2013.
- S. S. Stevens, "The surprising simplicity of sensory metrics," *Amer. Psychol.*, vol. 17, no. 1, p. 29, 1962.
- P. Patel, R. K. Ray, and M. Manivannan, "Power law based 'out of body' tactile funneling for mobile haptics," *IEEE Trans. Haptics*, vol. 12, no. 3, pp. 307–318, Aug. 2019.
- S. Dosen, S. Muceli, J. L. Dideriksen, J. P. Romero, E. Rocon, J. Pons, and D. Farina, "Online tremor suppression using electromyography and low-level electrical stimulation," *IEEE Trans. Neural Syst. Rehabil. Eng.*, vol. 23, no. 3, pp. 385–395, Jul. 2014.
- Z. Liao, J. V. S. Luces, and Y. Hirata, "Human navigation using phantom tactile sensation based vibrotactile feedback," *IEEE Robot. Autom. Lett.*, vol. 5, no. 4, pp. 5732–5739, Oct. 2020.
- H.-Y. Cho, S. H. Lee, T. S. In, K. J. Lee, and C. H. Song, "Effects of transcutaneous electrical nerve stimulation (TENS) on changes in postural balance and muscle contraction following muscle fatigue," *J. Phys. Therapy Sci.*, vol. 23, no. 6, pp. 899–903, 2011.
- J. Lee, H. Lee, A. Eizad, and J. Yoon, "Effects of using TENS as electro-tactile feedback for postural balance under muscle fatigue condition," in *Proc. 21st Int. Conf. Control, Autom. Syst. (ICCAS)*, Oct. 2021, pp. 1410–1413.
- H. Lee, A. Eizad, G. Lee, Y. Kim, and J. Yoon, "Development of haptic bracelets based arm swing feedback system for stroke survivors," in *Proc. 20th Int. Conf. Control, Autom. Syst. (ICCAS)*, Oct. 2020, pp. 1022–1025.
- B. K. Springer and D. M. Pincivero, "The effects of localized muscle and whole-body fatigue on single-leg balance between healthy men and women," *Gait Posture*, vol. 30, no. 1, pp. 50–54, Jul. 2009.
- E. Franzén, C. Paquette, V. Gurfinkel, and F. Horak, "Light and heavy touch reduces postural sway and modifies axial tone in Parkinson's disease," *Neurorehabilitation Neural Repair*, vol. 26, no. 8, pp. 1007–1014, Oct. 2012.
- South Korea. *Human Body Measurements*. Accessed: Feb. 28, 2022. [Online]. Available: <https://sizekorea.kr/3d-body/korean-standard-body-type/1>
- F. Mancini, A. Bauleo, J. Cole, F. Lui, C. A. Porro, P. Haggard, and G. D. Iannetti, "Whole-body mapping of spatial acuity for pain and touch," *Ann. Neurol.*, vol. 75, no. 6, pp. 917–924, Jun. 2014.
- J. B. Van Erp, "Presenting directions with a vibrotactile torso display," *Ergonomics*, vol. 48, no. 3, pp. 302–313, Feb. 2005.
- J. Xu, T. Bao, U. H. Lee, C. Kinnaird, W. Carender, Y. Huang, K. H. Sienko, and P. B. Shull, "Configurable, wearable sensing and vibrotactile feedback system for real-time postural balance and gait training: Proof-of-concept," *J. Neuroeng. Rehabil.*, vol. 14, no. 1, pp. 1–10, Dec. 2017.
- J. Han, S. Park, S. Jung, Y. Choi, and H. Song, "Comparisons of changes in the two-point discrimination test following muscle fatigue in healthy adults," *J. Phys. Therapy Sci.*, vol. 27, no. 3, pp. 551–554, 2015.
- Y. Konishi, P. McNair, and D. Rice, "TENS alleviates muscle weakness attributable to attenuation of Ia afferents," *Int. J. Sports Med.*, vol. 38, no. 3, pp. 253–257, Feb. 2017.
- D. Stanke, T. Duinte, and M. Rohs, "TactileWear: A comparison of electro-tactile and vibrotactile feedback on the wrist and ring finger," in *Proc. 11th Nordic Conf. Hum.-Comput. Interact., Shaping Experiences, Shaping Soc.*, Oct. 2020, pp. 1–13.
- R. Dickstein, Y. Laufer, and M. Katz, "TENS to the posterior aspect of the legs decreases postural sway during stance," *Neurosci. Lett.*, vol. 393, no. 1, pp. 51–55, Jan. 2006.
- G. Severini and E. Delahunt, "Effect of noise stimulation below and above sensory threshold on postural sway during a mildly challenging balance task," *Gait Posture*, vol. 63, pp. 27–32, Jun. 2018.
- S. E. Ross, "Noise-enhanced postural stability in subjects with functional ankle instability," *Brit. J. Sports Med.*, vol. 41, no. 10, pp. 656–659, Oct. 2007.

- [35] M. R. Afzal, H. Lee, A. Eizad, C. H. Lee, M.-K. Oh, and J. Yoon, "Effects of vibrotactile biofeedback coding schemes on gait symmetry training of individuals with stroke," *IEEE Trans. Neural Syst. Rehabil. Eng.*, vol. 27, no. 8, pp. 1617–1625, Aug. 2019.



**JUNYEONG LEE** received the B.S. degree in mechanical engineering from the School of Mechanical Engineering, Gwangju Institute of Science and Technology, Gwangju, South Korea, in 2022, where he is currently pursuing the Ph.D. degree with the School of Integrated Technology. In 2022, he joined the School of Integrated Technology, Gwangju Institute of Science and Technology. He has served as a Teaching Assistant with the Gwangju Institute of Science and Technology, in 2022. His current research interests include mechatronics, gait rehabilitation robots, and physical human–robot interaction.



**HOSU LEE** received the B.E. and M.S. degrees from the School of Mechanical Engineering, Gyeongsang National University, Jinju, South Korea, in 2014 and 2016, respectively, the Ph.D. degree from Gyeongsang National University, in 2017, and the Ph.D. degree from the Department of Mechatronics, Gwangju Institute of Science and Technology (GIST), Gwangju, South Korea, in 2022. From 2016 to 2017, he was a Researcher with Gyeongsang National University. He worked as a Teaching Assistance of mechatronics and robotics at GIST, from 2019 to 2021. He is currently working as a Postdoctoral Researcher at the Intelligent Medical Robotics Laboratory and the Cognition and Intelligence Laboratory, GIST. His current research interests include rehabilitation robotics, haptic feedback interfaces, cable driven parallel robot (CDPR), and locomotion interface.



**AMRE EIZAD** received the B.E. and M.S. degrees in mechatronics engineering from Air University, Islamabad, Pakistan, in 2009 and 2011, respectively, and the Ph.D. degree in mechanical and aerospace engineering from Gyeongsang National University, Jinju, Republic of Korea, in 2020. From 2009 to 2011, he was a Laboratory Engineer with the Department of Mechatronics Engineering, Air University, where he later served as a Lecturer, from 2011 to 2016. From 2020 to 2022, he was a Postdoctoral Researcher at the Intelligent Medical Robotics Laboratory, Gwangju Institute of Science and Technology. He is currently working as a Postdoctoral Researcher at the Center for Intelligent and Interactive Robotics, Korea Institute of Science and Technology, Republic of Korea. His research interests include the development of rehabilitation systems and assistive devices.



**JUNGWON YOON** (Member, IEEE) received the Ph.D. degree in mechatronics from the Gwangju Institute of Science and Technology, Gwangju, South Korea, in 2005. From 2001 to 2002, he was a Visiting Researcher at the Virtual Reality Laboratory, Rutgers University, Piscataway, NJ, USA, and a Visiting Fellow at the Functional and Applied Biomechanics Section, Department of Rehabilitation Medicine, Clinical Center, National Institutes of Health, Bethesda, MD, USA, from 2010 to 2011. He was also a Senior Researcher at the Electronics Telecommunication Research Institute (ETRI), Daejeon, South Korea. From 2005 to 2017, he was a Professor with the School of Mechanical and Aerospace Engineering, Gyeongsang National University, Jinju, South Korea. In 2017, he joined the School of Integrated Technology, Gwangju Institute of Science and Technology (GIST), Gwangju, South Korea, where he is currently a Professor. Since 2019, he has been the Director of the Research Center for Nanorobotics in Brain (RCNB), GIST. He is also a principal project director in several large-scale research projects supported by the South Korea Governments in the themes of brain stimulation, drug delivery, and hyperthermia using nano robotics. He has authored or coauthored more than 200 peer-reviewed international journals and conference papers. His current research interests include magnetic particle imaging, bio-nano robot control, and rehabilitation robots. He was a Technical Editor of *IEEE/ASME TRANSACTIONS ON MECHATRONICS* and an Associate Editor of *Frontiers in Robotics and AI*.

...